

## Modulation of the Porphyrin Inner Proton Exchange Rates by the Steric Effects of Bridge Substitution

Héctor García-Ortega,<sup>†</sup> Joaquim Crusats,<sup>†</sup> Miguel Feliz,<sup>‡</sup> and Josep M. Ribó<sup>\*†</sup>

Department of Organic Chemistry, University of Barcelona, Martí i Franquès 1,  
08028-Barcelona, Catalonia, Spain, and Serveis Científicotècnics, University of Barcelona,  
Josep Samitier 5, 08028-Barcelona, Catalonia, Spain

jmr@qo.ub.es

Received December 10, 2001

The tautomeric equilibria and H–N proton transfer taking place in the nonsymmetrically substituted water-soluble 2-sulfonato-5,15-bis(4-sulfonatophenyl)porphyrin (**1**) and in its 10-bromo-substituted derivative (**2**) were analyzed by NMR methods: <sup>1</sup>H and <sup>13</sup>C spectroscopies and heteronuclear multiple bond correlation (HMBC) and heteronuclear single quantum coherence (HSQC) <sup>1</sup>H–<sup>13</sup>C and <sup>1</sup>H–<sup>15</sup>N techniques. The existence of preferred pathways of H–N transfer was detected. The conclusions are rationalized by taking into account the effect partial meso-substitution exerts on the relative energies of the different cis-tautomer intermediates involved in the tautomerism. These results underline the experimental consequences stemming from the nonequivalence in porphyrins between the 'tautomeric interconversion' and 'proton transfer' terms, when observed by NMR techniques, as a consequence of the existence of two pairs of degenerate tautomers and transformation pathways.

### Introduction

Porphyrinoids are being developed as photosensitizers for photodynamic therapy.<sup>1</sup> The study of their tautomeric behavior is thus relevant because of its role in their photochemical and photophysical properties. Leaving aside the pure scientific aspects of the tautomerism,<sup>2</sup> there is also interest in their potential practical applications in molecular memory storage devices, especially when the tautomers show unequal ground and excited state energies or differences in oscillator strengths.<sup>3</sup> In addition, porphyrins are attracting the attention of materials chemists owing to the singular electronic and optical properties of their chromophoric systems, which make them suitable for nonlinear optics and optical visible region hole-burning applications.<sup>4</sup>

The tautomeric equilibria of porphyrins<sup>5</sup> and their kinetics can be polarized through the substitution of the porphyrin periphery.<sup>6</sup> It has been established that ir-

regular substitution patterns in nonsymmetric porphyrins can lead to two distinguishable paths for the tautomeric process.<sup>7</sup> But, similar studies on the proton exchange rates of partially meso-substituted porphyrins, which can show noteworthy kinetic properties, could be further revealing and are still lacking. This information would be particularly useful in order to interpret the experimental evidence currently available, independently noticed by different authors in unrelated works, regarding atypical proton exchange rates in certain porphyrins.<sup>8</sup>

Water-soluble porphyrins, on the other hand, are being proposed as molecular building blocks for the supramolecular engineering of soft materials and nanodevices.<sup>9</sup> Moreover, their high polarity makes them conveniently dispersible into a wide range of functional polymeric films. We have recently reported on the synthesis, characterization, and reactivity of various nonsymmetrically substituted water-soluble porphyrins, among them, the sodium salts of 2-sulfonato-5,15-bis(4-sulfonatophenyl)porphyrin (**1**) and 10-bromo-2-sulfonato-5,15-bis(4-sulfonatophenyl) porphyrin (**2**) (Scheme 1).<sup>10</sup> Substitution with a sulfonato group at a  $\beta$ -position (C-2) is expected to polarize the tautomeric equilibrium of the NH exchange. Moreover, these two porphyrins show irregular substitution patterns in their meso-positions, which may substantially affect the H–N pathways of proton transfer

\* To whom correspondence should be addressed.

<sup>†</sup> Department of Organic Chemistry.

<sup>‡</sup> Serveis Científicotècnics.

(1) Bonnett, R. *Chemical Aspects of Photodynamic Therapy*; Advanced Chemistry Texts, Gordon and Breach Science Publishers: The Netherlands 2000.

(2) (a) Ghosh, A. In *Porphyrin Handbook*; Kadish, K. M., Smith, K. M., Guillard, R., Eds.; Academic Press: San Diego, CA, 2000; Vol. 7, Chapter 47, pp 16–21. (b) Medforth, C. J. In *Porphyrin Handbook*; Kadish, K. M., Smith, K. M., Guillard, R., Eds.; Academic Press: San Diego, CA, 2000; Vol. 5, Chapter 35, pp 12–16 and pp 61–63. (c) Ghosh, A. *Acc. Chem. Res.* **1998**, *31*, 189–198.

(3) (a) Drobizhev, M.; Sigel, C.; Rebane, A. *J. Lumin.* **2000**, *86*, 391–397. (b) Starukhin, A.; Shulga, A.; Wild, U. P. *J. Lumin.* **2001**, *93*, 81–92.

(4) Heldt, J.; Gormin, D.; Kasha, M. *Chem. Phys.* **1989**, *136*, 321–334.

(5) (a) Claramunt, R. M.; Elguero, J.; Katritzky, A. R. *Adv. Heterocycl. Chem.* **2000**, *77*, 1–50. (b) Furuta, H.; Ishizuka, T.; Osuka, A.; Dejima, H.; Nakagawa, H.; Ishikawa, Y. *J. Am. Chem. Soc.* **2001**, *123*, 6207–6208.

(6) (a) Crossley, M. J.; Harding, M. M.; Sternhell, S. *J. Am. Chem. Soc.* **1986**, *108*, 3608–3613. (b) Crossley, M. J.; Harding, M. M.; Sternhell, S. *J. Org. Chem.* **1992**, *57*, 1833–1837.

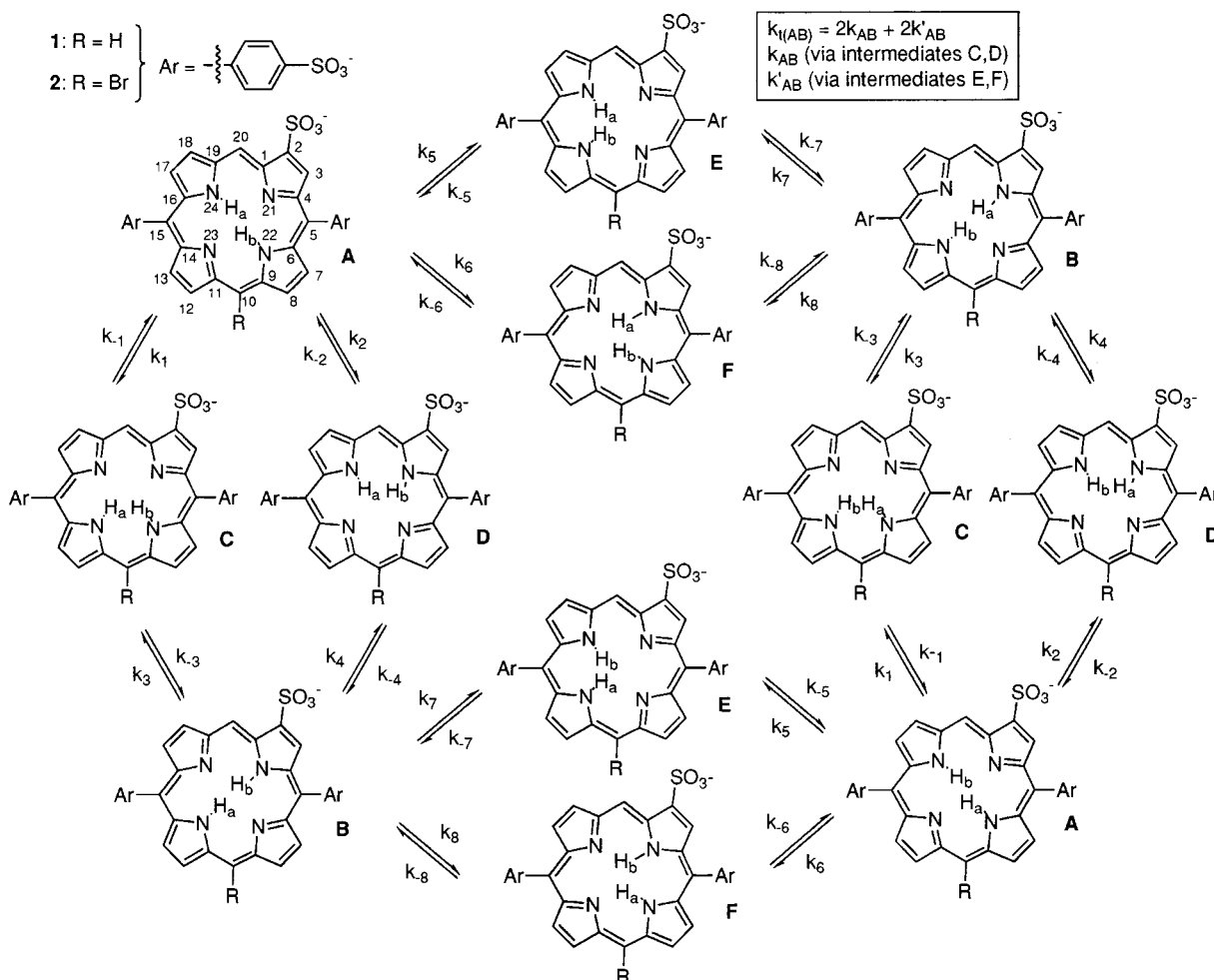
(7) Crossley, M. J.; Field, L. D.; Harding, M. M.; Sternhell, S. *J. Am. Chem. Soc.* **1987**, *109*, 2335–2341.

(8) (a) Sessler, J. L.; Johnson, M. R.; Creager, S. E.; Fetting, J. C.; Ibers, J. A. *J. Am. Chem. Soc.* **1990**, *112*, 9310–9329. (b) Asakawa, M.; Toi, H.; Aoyama, Y.; Ogoshi, H. *J. Org. Chem.* **1992**, *57*, 5796–5798. (c) Shaw, S. J.; Shanmugathan, S.; Clarke, O. J.; Boyle, R. W.; Osborne, A. G.; Edwards, C. J. *J. Porph. Phthal.* **2001**, *5*, 575–581.

(9) (a) Ribó, J. M.; Rubires, R.; El-Hachemi, Z.; Farrera, J. A.; Campos, L.; Pakhomov, G. L.; Vendrell, M. *Mater. Sci. Eng. C* **2000**, *11*, 107–115. (b) Simon, J.; Bassoul, P. *Design of Molecular Materials, Supramolecular Engineering*; John Wiley and Sons: Chichester, England, 2000.

(10) García-Ortega, H.; Ribó, J. M. *J. Porph. Phthal.* **2000**, *4*, 564–568.

Scheme 1



in their inner cavity. In the present paper, by means of various NMR spectroscopic methods, and taking advantage of the magnetic nonequivalences of the four nitrogen atoms raised by the  $\beta$ -sulfonic substituent in compounds **1** and **2**, we analyze the effect of the steric hindrances caused by bulky substituents in the bridge positions upon the porphyrin tautomerism.

### Results and Discussion

**$^{13}\text{C}$  NMR.** All carbon atoms of porphyrin **1** could be matched to well-resolved narrow peaks of its  $^{13}\text{C}$  NMR spectrum obtained at room temperature in DMSO and DMF solutions. Assignments were made with the aid of heteronuclear correlations obtained in  $^1\text{H}$ - $^{13}\text{C}$  HSQC and  $^1\text{H}$ - $^{13}\text{C}$  HMBC experiments (see Supporting Information). The chemical shifts of the carbon atoms at the  $\alpha$  position in the five-membered rings were those expected for an  $\alpha$ -pyrrolic position in the case of C6, C9, C16, and C19 (141–142 ppm), whereas for C1, C4, C11, and C14 their values were those characteristic of  $\alpha$ -pyrroleninic type (145–152 ppm). This points to the presence of **1A** (Scheme 1) as the only tautomer or, alternatively, to a fast equilibrium between **1A** and **1B** strongly shifted toward the former.

In the case of porphyrin **2**, the detected signals could be assigned to their corresponding carbon atoms on the basis of their  $^1\text{H}$ - $^{13}\text{C}$  HSQC and  $^1\text{H}$ - $^{13}\text{C}$  HMBC correlations, performed at room temperature in DMSO and DMF. Notably, the quaternary  $\alpha$ -carbon atoms, with the

sole exception of C1, were missing in the spectrum. Nevertheless, the chemical shifts for the detected signals again pointed to the structure of the **2A** tautomer, in a similar way to what occurred in **1**. For instance, the C1 signal in **1** and **2** only differed in 0.3 ppm, and its chemical shift of  $\sim 153$  ppm is characteristic of a cyclic iminic carbon atom. When the spectrum was recorded at 323 K, the signals corresponding to several of the missing  $\alpha$ -carbon atoms (C14, C4, and C6) could be detected, though with variable bandwidths, and there were no substantial changes in the chemical shifts for the rest of the signals. Thus, the inability to detect the  $\alpha$ -carbon atoms in the  $^{13}\text{C}$  NMR spectrum of **2** must be attributed to line-broadening below the detection limit of the experiment due to coalescence of carbon peaks appearing at different chemical shifts in each tautomer. The carbon atoms with small chemical shift differences between each tautomeric form will be above coalescence at lower temperatures. This is the case of C1 in **2** which is already detected at room temperature and whose small chemical shift difference between tautomers is probably originated by the C1 proximity to the  $\beta$ -sulfonato group in B.

The disappearance of the  $\alpha$ -carbon atom signals in certain porphyrins has been previously attributed to the rate of the N–H exchange.<sup>11</sup> It has recently been reported that 5,15-diaryl-substituted porphyrins show sharp  $\alpha$ -

(11) Abraham, R. J.; Hawkes, G. E.; Smith, K. M. J. *Chem. Soc. Perkin Trans. 2* 1975, 627–634.

and  $\beta$ -carbon atom peaks, similar to those of **1**, as a consequence of a faster proton exchange rate.<sup>8c</sup> Contrarily, 10-halogeno-5,15-diphenyl-substituted porphyrins, similar to compound **2**, were found to show broad  $\alpha$ -carbon signals, thereby pointing again to moderate exchange rates. Hence, from the recorded <sup>13</sup>C NMR data, we can confirm the effect the substitution at C10 has on the rate of tautomeric exchange of 5,15-diphenylporphyrins, and we can also conclude that the A form constitutes the predominant tautomer. The same results suggest that the  $\beta$ -substitution next to a free meso position of the porphyrin ring (i.e.  $-\text{O}_3\text{S}-\text{C}2$ , in **1** and **2**) has only a small influence on its kinetic behavior concerning the NH tautomerism. At this stage, an oversimplified consideration of the mechanism for the tautomer exchange, solely made on the basis of steric hindrance considerations, might wrongly conclude that the substitution at C10 implies a concomitant decrease of the proton transfer rates. As we show below, this is not necessarily so.

**<sup>1</sup>H NMR.** The <sup>1</sup>H NMR spectra of substances **1** and **2** showed a unique set of C–H signals as is to be expected for the existence of a single substance or, alternatively, a fast interconversion between both tautomeric forms. The whole group of C–H signals in the <sup>1</sup>H NMR spectra of porphyrins **1** and **2**, in DMSO and DMF, were unambiguously assigned through the study of the cross-peaks obtained in NOESY and COSY experiments (see Supporting Information). For both substances **1** and **2**, the analysis of the detected cross-peaks between the C–H signals and the N–H protons allowed us to identify the A forms depicted in Scheme 1 as the very predominant tautomer (the form in which the sulfonato group is not, as expected, directly substituted on the aromatic delocalization pathway of the porphyrin  $\pi$  system<sup>6b</sup>). At room temperature, compound **1** showed two N–H signals, which were matched to the N22–H and N24–H pairs on the basis of their long distance couplings with C7–H, C8–H, and C17–H, C18–H, respectively (Figure 1 and Supplementary Information). At the same temperature, compound **2** showed a single signal for both inner NH protons which was coupled to C7–H, C8–H, C17–H, and C18–H. Notwithstanding, at this point we cannot exclude the presence of the minor B tautomers as a consequence of the failure to detect their corresponding cross-peaks in the COSY experiments, as we demonstrate later in this work. The number of N–H signals at room temperature in the case of **1** evidences the confinement of each proton ( $\text{H}_a$  and  $\text{H}_b$  in Scheme 1) in a different half of the porphyrin inner ring at the NMR time scale. This is contrary to the behavior exhibited in **2**. In other words, in the <sup>1</sup>H NMR experiments we detect a slower proton exchange rate for **1** than for **2**.

Variable-temperature <sup>1</sup>H NMR experiments allowed us to study the exchange of  $\text{H}_a$  and  $\text{H}_b$  (Figure 2, Table 1). The two different H–N signals recorded for **1** collapsed into one signal above a coalescence temperature of 323 K in DMSO and 328 K in DMF. On the other hand, the single NH signal recorded for **2** split in two below 283 K. At room temperature, the trans-(H–N21, H–N23) and trans-(H–N22, H–N24) tautomers A and B interconvert rapidly making their individual detection by <sup>1</sup>H NMR spectroscopic methods impossible. Accordingly, the recorded spectra showed averaged NH resonance signals on the NMR time-scale as a consequence of fast exchange, confirming the existence of the tautomeric process. In addition, the A and B tautomers are energetically non-

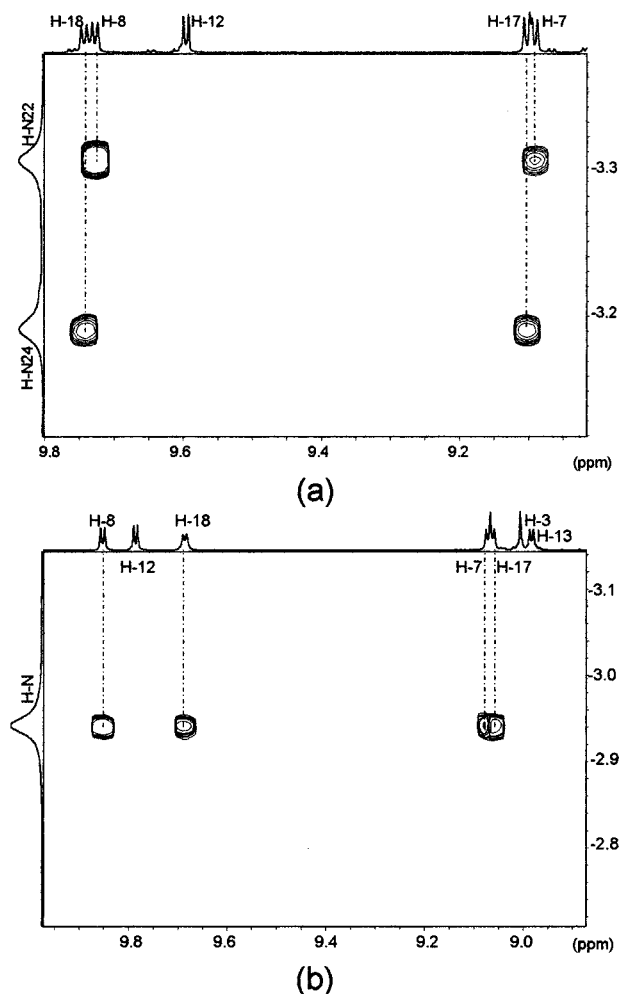


**Figure 1.** <sup>1</sup>H NMR (600 MHz) COSY experiments at 298 K for **1** in DMSO-*d*<sub>6</sub> (a) and **2** in DMF-*d*<sub>7</sub> (b) showing the cross-peaks between H–N and the protons on the  $\beta$ -carbon atoms.

degenerate and are thus present in different amounts in the equilibrium. This also affects the overall temperature dependence of the averaged chemical shifts detected for the N–H signals. Further to these observations, and owing to the chemical nonequivalence of the four nitrogen sites in porphyrins **1** and **2**, at low enough temperatures a second splitting of each N–H peak into two signals of unequal intensities, in accordance with the molar ratio of each tautomer in the equilibrium, is expected a priori. However, the solubility properties of substances **1** and **2** and the solidification point of the solvents limited the experimental range of temperatures which could be tested. Even at the lowest temperature we could reach, 250 K in DMF, we were unable to detect two separate pairs of signals corresponding to the nondegenerate tautomers A and B.

The appearance of two N–H signals of equal intensities in Figure 2 can be readily interpreted by considering the existence of the two different pathways for the A to B tautomerism depicted in Scheme 1, with only one of these pathways allowing fast exchange on the NMR time-scale. The obtained data show that the tautomeric interconversion process of porphyrin **1**, even at room temperature, is confined via a single path at the <sup>1</sup>H NMR time scale. In the case of **2**, a similar behavior occurs at lower temperatures, albeit the total exchange rate constant between form A and form B is slower than that for **1**. At



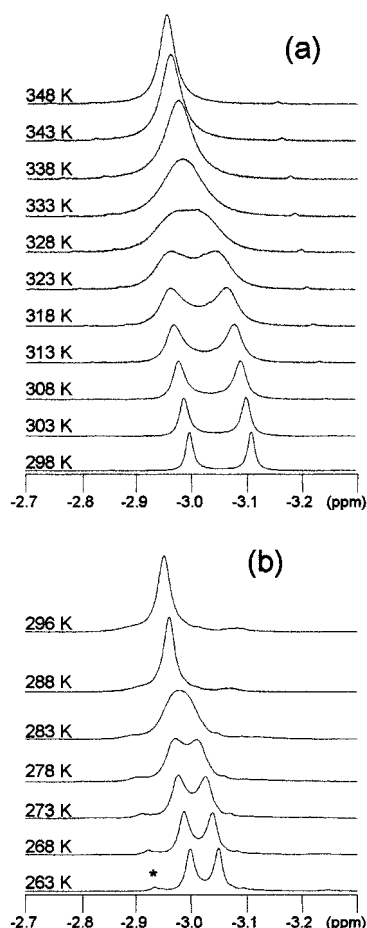


**Figure 2.** NH section of the  $^1\text{H}$  NMR (600 MHz) spectrum of **1** (a) and **2** (b) in  $\text{DMF}-d_7$  at various temperatures (\* impurity).

**Table 1. Rate Constants of the NH Tautomerism Determined at the Total Coalescence Temperature**

compd	DMSO- $d_6$			DMF- $d_7$		
	$T_c$ (K)	$k_{TC}$ ( $\text{s}^{-1}$ )	$\Delta G_{TC}^\ddagger$ (kJ/mol)	$T_c$ (K)	$k_{TC}$ ( $\text{s}^{-1}$ )	$\Delta G_{TC}^\ddagger$ (kJ/mol)
<b>1</b>	$323 \pm 2$	$150 \pm 19$	$65.9 \pm 0.8$	$328 \pm 2$	$150 \pm 18$	$66.9 \pm 0.8$
<b>2</b>	$<293$			$283 \pm 2$	$64 \pm 8$	$59.4 \pm 0.8$

this point a question arises as to whether the  $k_{AB} > k'_{AB}$  or, conversely,  $k_{AB} < k'_{AB}$  (Scheme 1). In other words, which is the favored path for the proton-transfer process?

**$^1\text{H}$ – $^{15}\text{N}$  NMR.** To answer the above question, two-dimensional experiments in DMSO and DMF at the natural abundance of  $^{15}\text{N}$  were performed within the  $^1\text{H}$ – $^{15}\text{N}$  heteronuclear multiple bond correlation (HMBC) and the  $^1\text{H}$ – $^{15}\text{N}$  heteronuclear single quantum coherence (HSQC) NMR pulse sequence methods.

In the case of porphyrin **1**, four different nitrogen signals were detected in two pairs, with only very small chemical shift differences between the members of each pair (Figure 3 and Supplementary Information). The recorded chemical shifts, together with the chemical shift differences between pairs of 47 and 35 ppm in DMSO and DMF, respectively, point to the presence of a major tautomer in equilibrium with its minor counterpart.<sup>12</sup> Each nitrogen atom could be unequivocally matched to its  $^{15}\text{N}$  NMR signal by the  $^1\text{H}$ – $^{15}\text{N}$  heteronuclear multiple

bond correlation measurements shown in Figure 3: Nitrogens N22 and N23 showed intense cross-peaks with H10 and nitrogens N21 and N24 with H20. Supporting evidence for these assignments, along with further information leading to complete atom discrimination, were obtained by additional correlations of each nitrogen atom with the protons located at the  $\beta$ -positions of the porphyrin periphery (see Figure 3 and Supporting Information). Thus, from the information obtained in the HMBC experiment we can assign the pair of intense signals appearing at higher fields to N22 and N24, and the pair of lower intensities to N21 and N23.

By means of 2D  $^1\text{H}$ – $^{15}\text{N}$  heteronuclear single quantum coherence NMR correlation measurements, each inner proton showed strong  $^1\text{H}$ – $^{15}\text{N}$  one-bond correlations with opposite nitrogen atoms of the porphyrin core (Figure 4), in agreement with the existence of the expected most stable trans-tautomer. We detected cross-peaks between the H–N at  $-3.18$  ppm and the nitrogens at 165.1 and 212.0 ppm, and between the H–N at  $-3.29$  ppm and the nitrogens at 165.5 and 212.8 ppm. We cannot exclude at this point the detection of indirect cross-peaks originating from  $\text{H}_a$  and proton  $\text{H}_b$  interconversion after the refocusing period of the HSQC pulse sequence.<sup>13</sup> Nevertheless, the high symmetry of the detected cross-peaks at several experimental conditions in DMSO and DMF, the positions of whose maximum heights correlate fairly well with the chemical shifts detected for the nitrogen atoms in the  $^1\text{H}$ – $^{15}\text{N}$  HMBC NMR experiment, point toward their absence. Whatever the case may be, the possible contribution of these additional low intense signals to the recorded cross-peaks would not affect the inferred conclusion. Moreover, since the cross-signal intensities are sensitive to the polarization of the tautomeric equilibrium, they point to a high proportion of one of the tautomers in the mixture, as anticipated for a nonsymmetric porphyrin and inferred from the  $^1\text{H}$  and  $^{13}\text{C}$  NMR experiments. Clearly, the stronger correlations correspond to N22 and N24, whose averaged-chemical-shift pyrrolic character is associated to an equilibrium shift to tautomer A. The volume integration of the cross-signals points to  $84 \pm 3\%$  of tautomer A and  $16 \pm 3\%$  of tautomer B in DMSO and to  $87 \pm 3\%$  (A):  $13 \pm 3\%$  (B) in DMF. These last results are also in agreement with the A/B ratios inferred through the chemical shift differences detected between the time-averaged pyrrolic and pyrroleninic nitrogen atoms in **1**.

With this information at hand, the proton transfer confinement detected in porphyrin **1** at room temperature could be addressed. The matching of the most intense signals with those of the second pair of weaker correlations, corresponding to the minor tautomer B, allowed us to determine the favored path for the tautomeric process in **1** (Figure 4). The matching unambiguously sets  $\text{H}_a$  to N24 (strong) and N23 (weak) and  $\text{H}_b$  to N22 (strong) and N21 (weak). These assignments show that the slow  $\text{H}_a$  to  $\text{H}_b$  interconversion is due to  $k'_{AB} < k_{AB}$  (Scheme 1), thereby pointing to a faster exchange through the *meso*-phenyl-substituted positions than through the alternatively available unsubstituted ones. The same heteronuclear NMR experiments performed on **2** did not afford any detectable correlations, even at 328 K. This negative

(12) Chemical shifts of about 134 and 240 ppm can be expected for the pyrrolic and pyrroleninic nitrogen atoms in the porphyrin ring, i.e., a difference of more than 100 ppm. See page 37 of reference 2b.

(13) (a) Helaja, J.; Montforts, F.-P.; Kilpelainen, I.; Hynninen, P. H. *J. Org. Chem.* **1999**, *64*, 432–437. (b) Helaja, J.; Stapelbroek-Mollmann, M.; Kilpelainen, I.; Hynninen, P. H. *J. Org. Chem.* **2000**, *65*, 3700–3707.

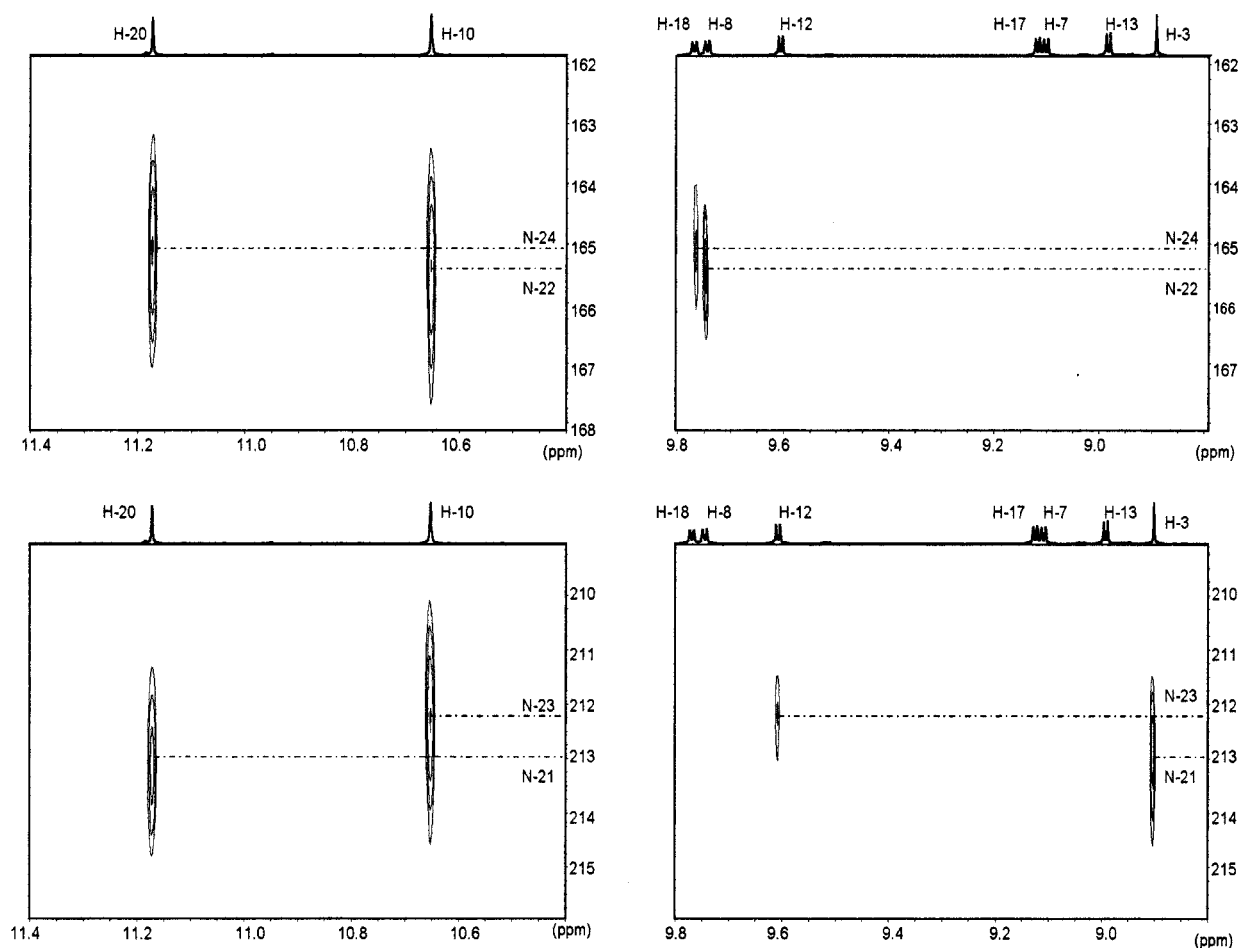


**Figure 3.**  $^1\text{H}$ – $^{15}\text{N}$  HMBC (600 MHz) cross-peaks for **1** in  $\text{DMSO}-d_6$  at 298 K.

result must be attributed to low sensitivity. This is probably a consequence of the broadening of the nitrogen signals beyond the detection limit of the experiment as a consequence of their coalescence between the pyrrolic and pyrrolenic state.

**Tautomeric A to B Interconversion and Proton Exchange Rates.** Porphyrin trans-NH-tautomers present the singularity of existing as degenerate species: there are four identical tautomers in the case of symmetrically substituted macrocycles; and two different pairs for the nonsymmetrically substituted ones, like **1** and **2** (tautomers A and B, Scheme 1). Obviously, when considering the interconversion among these NH tautomers, the existence of the corresponding degenerate reaction pathways has to be kept in mind. Hence, the A to B interconversion for **1** and **2** depends on the total rate constant  $k_{\text{t(AB)}} = 2k_{\text{AB}} + 2k'_{\text{AB}}$ , regardless of the relative magnitude of  $k_{\text{AB}}$  to  $k'_{\text{AB}}$ . As discussed below, the proton exchange mechanism in porphyrins takes place via the intermediate cis-NH-tautomers.<sup>14</sup> In consequence of this, the routes depicted in Scheme 1 are pairs of specific reaction pathways. In the case of **1** and **2**, there exist two nondegenerate pairs of paths for both  $k_{\text{AB}}$  and  $k'_{\text{AB}}$  depending on which of the protons initiates the transfer.

The total rate constant [ $k_{\text{t(AB)}}$ ] is the limiting factor governing whether the signals of the  $^{13}\text{C}$  atoms in both tautomers can be distinguished through their chemical shifts at the NMR time scale or, on the other hand, appear at identical chemical shifts corresponding to their averaged signal according to their molar fractions in the equilibria. In contrast, the  $^1\text{H}$  NMR time scale for the N–H signals depends on both  $k_{\text{AB}}$  and  $k'_{\text{AB}}$ . If  $2k_{\text{AB}}$  and  $2k'_{\text{AB}}$  are small enough, four N–H signals can be expected, whereas for higher enough values of  $2k_{\text{AB}}$  and  $2k'_{\text{AB}}$ , only one N–H signal will be observed. Taking these last considerations into account and comparing the obtained spectral data for **1**, it is self-evident that at room temperature and under our tested conditions,  $k_{\text{AB}}$  is high enough, and  $k'_{\text{AB}}$  low enough, to allow the detection by  $^1\text{H}$  NMR spectroscopy of two distinguishable NH signals. In addition  $k_{\text{t(AB)}}$  also is high enough to allow the detection of the  $\alpha$ - $^{13}\text{C}$  atoms above their coalescence temperature. In comparison, the bromine substitution at C10 (**2**) results in an increase in  $k'_{\text{AB}}$  (detected through the  $^1\text{H}$ –N signals and HSQC experiments), but there is also a decrease in  $k_{\text{t(AB)}}$  ( $\alpha$ - $^{13}\text{C}$  atoms signals of **1** vs of **2**; see above). In **1**, there is fast proton exchange taking place via the substituted meso positions ( $k_{\text{AB}} > k'_{\text{AB}}$ ). In **2**, the bromination at C10 results in an increase in  $k'_{\text{AB}}$  ( $k'_{\text{AB}}$  for **2** >  $k'_{\text{AB}}$  for **1**), but also in a decrease in  $k_{\text{AB}}$  ( $k_{\text{AB}}$  for **2** <  $k_{\text{AB}}$  for **1**, since  $k_{\text{t(AB)}}$  for **1** >  $k_{\text{t(AB)}}$  for **2**).

The preference for determinate paths for the proton transfer can be rationalized by considering the established mechanism for the tautomerism. It is currently

(14) (a) Maity, D. K.; Bell, R. L.; Truong, T. N. *J. Am. Chem. Soc.* **2000**, *122*, 897–906. (b) Reimers, J. R.; Lü, T. X.; Crossley, M. J.; Hush, N. S. *J. Am. Chem. Soc.* **1995**, *117*, 2855–2861. (c) Braun, J.; Schlabach, M.; Vehrle, B.; Köcher, M.; Vogel, E.; Limbach, H. H. *J. Am. Chem. Soc.* **1994**, *116*, 6593–6604, and references therein. (d) Braun, J.; Limbach, H.-H.; Williams, P. J.; Morimoto, H.; Wemmer, D. E. *J. Am. Chem. Soc.* **1996**, *118*, 7231–7232.

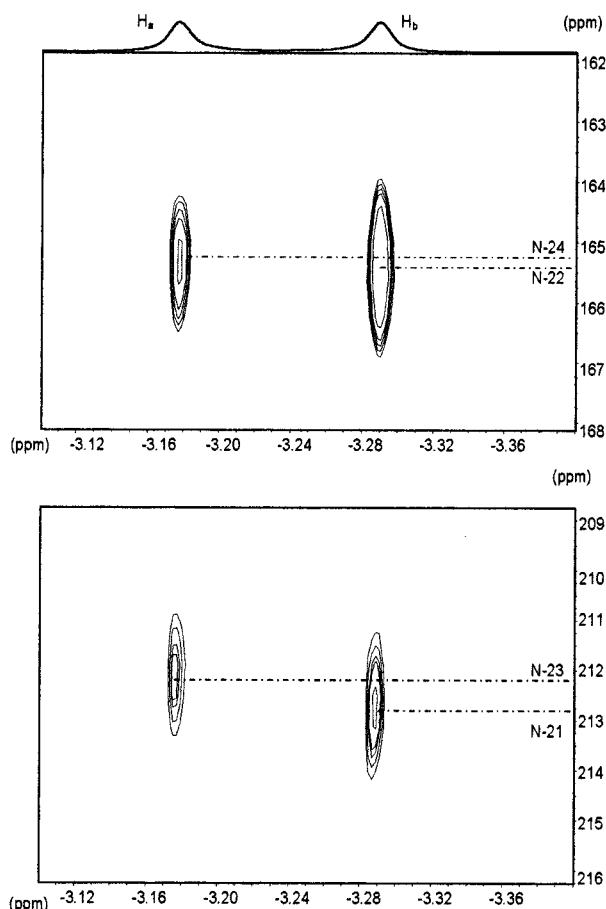


**Figure 4.**  $^1\text{H}$ – $^{15}\text{N}$  HSQC (600 MHz) cross-peaks for **1** in  $\text{DMSO}-d_6$  at 298 K.

accepted that N–H migration in porphyrins occurs via a stepwise mechanism through the cis-tautomer intermediates (Scheme 1 and Figure 5) rather than by means of a concerted mechanism involving synchronous migration of both hydrogen atoms.<sup>14</sup> In this way, the A to B interconversion takes place through two consecutive single N–H transfers. In nonsymmetrically substituted porphyrins, such as **1** and **2**, there are two degenerate sets of four different cis-tautomers. Therefore the rate constants  $k_{\text{AB}}$  and  $K_{\text{AB}}$  arise from two pathways, which are not necessarily degenerate. However, the relatively high difference in energies between cis- and trans-tautomers does not allow the direct detection of the cis-tautomers, and the relative contribution of each pathway on  $k_{\text{AB}}$  and  $K_{\text{AB}}$  cannot be straightforwardly determined through indirect methods. Simple force-field calculations<sup>15</sup> performed on simplified models give an insight into the complexity of the effects exerted by meso substitution on the proton-transfer pathways. In the case of symmetric compounds, comparing porphyrin and tetraphenylporphyrin, the energy gap value between the trans- and cis-tautomers is similar in both cases. That is, the steric hindrance effects are analogous in the trans- and cis-tautomers. On the other hand, partial meso substitution shows strong different effects on the cis-

(15) Simplifications on the structure of **1** and **2** (only using *meso*-phenyl substituents) should be made for the sake of accuracy of the available parametrization of the used force field (Experimental Section). In any event, despite the inaccuracy of the values obtained with these calculations, they roughly illustrate the sort of effects exerted by the meso substitution.

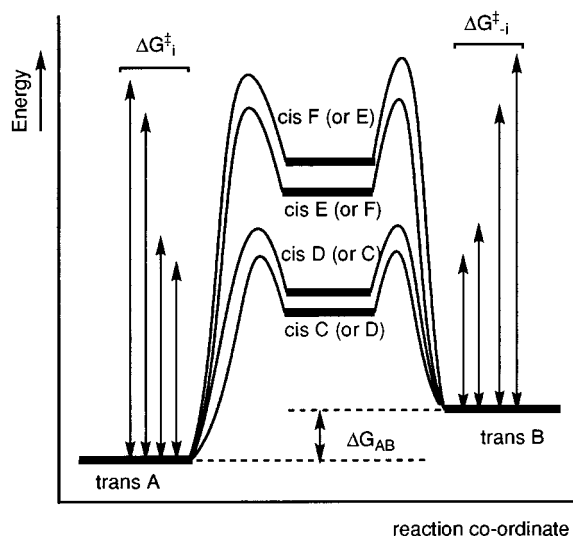


**Figure 5.** Coordinate reaction model of one of the degenerate pairs of pathways resulting in the interconversion between the trans tautomers in the case of nonsymmetric substitution of the porphyrin ring (e.g. cases of compounds **1** and **2**, see text). The relative values between  $\Delta G_i^\ddagger$  and  $\Delta G_{-i}^\ddagger$ , as well as the energy differences between C and D or E and F, cannot be inferred from the experimental results (see text).

tautomers, i.e., it increases or decreases the energy of determinate pathways in relation to the system with equal substitution at the four bridges. The monosubstituted 5-phenylporphyrin discriminates between  $k_{\text{AB}}$  and  $K_{\text{AB}}$  through the energy differences between its various cis- and trans-tautomers. For instance, the situation experimentally found in the tautomerism of monoaryl-substituted porphyrins reported by Ogoshi<sup>8b</sup> can be understood within this context. Next, 5,15-diphenylporphyrin shows strong differences between its two types of cis-tautomers. This agrees with the preferred proton-transfer pathway via the substituted meso positions experimentally detected for **1** in the present paper. Finally, the trisubstitution exerted by bromination at C10 creates energy changes in the cis-tautomers that validate the decrease in the proton-transfer rates through the phenyl-substituted positions due to the energy increase in one of the cis-intermediates of the two possible pathways contributing to  $k_{\text{AB}}$ . A general conclusion of these simple calculations is that the more stable cis-tautomers correspond to those structures in which the planarity of the bis(azafulvenic) moiety is less disturbed. Depending on the meso-substitution pattern the A and B trans-tautomers can be degenerate in symmetrically  $\beta$ -substituted porphyrins, yet the energy differences among cis-tautomers may strongly favor determinate proton-transfer routes. Altogether, these results suggest that even though the effect of meso-substitution on the individual pathways can be substantial, the total tautomeric rate constant  $k_{\text{t(AB)}}$  may be almost unaffected. In this regard, it is worth recalling at this point the cyclic nature of the porphyrin skeleton and the N–H confinement within its inner cavity. The N–H protons of partially meso-substituted porphyrins can be confined in different halves of the macrocycle ( $k_{\text{AB}} \gg K_{\text{AB}}$ ) without substantial change in the total tautomerism rate  $k_{\text{t(AB)}}$  between trans-tautomers. This peculiar tautomeric behavior, which is apparently a general feature of the substitution pattern,<sup>8a</sup> must not mislead us to the wrong

conclusion that the tautomer interconversion [ $k_{\text{t(AB)}}$ ] is slower than usual when the contrary may in fact be the case. 5,15-Diphenylporphyrins can be taken as the paradigmatic example of this particular effect, whose difference between  $k_{\text{AB}}$  and  $k'_{\text{AB}}$  can be easily overlooked in symmetrically substituted systems.

### Experimental Section

The synthesis of 2-sulfonato-5,15-bis(4-sulfonatophenyl)-porphyrin trisodium salt (**1**) and 10-bromo-2-sulfonato-5,15-bis(4-sulfonatophenyl)porphyrin trisodium salt (**2**) has been previously described.<sup>10</sup>

The NMR experiments ( $^{13}\text{C}$ , gCOSY,  $^1\text{H}$ – $^{13}\text{C}$  gHSQC) of **1** and **2** were recorded at 24 °C on a 600 MHz spectrometer in DMSO and DMF. The long-range correlation experiments (gHMBC) were performed using a multiple bond constant of 8 Hz and one bond coupling constant of 140 Hz. The gCOSY<sup>16</sup> and gHMBC<sup>17</sup> data were collected in absolute value and the gHSQC<sup>18</sup> experiments were acquired in phase using the hyper complex method. The spectral width was 8000 Hz in the proton dimension and 20120 Hz in the  $^{13}\text{C}$  dimension. Eight accumulations and 256 increments were carried out in the COSY experiments and 32 accumulations and 200 increments in the heterocorrelation experiments. In all experiments a linear prediction was applied to extend the data to double the number of data points in the FID. The  $^1\text{H}$ – $^{15}\text{N}$  NMR heteronuclear

correlation spectra were recorded from a 30 mM solution of **1** and **2** in DMSO and DMF in a Bruker Avance 600 MHz spectrometer. The coherence selection in HMBC<sup>17</sup> was achieved using gradients in  $z$ . In the gHMBC and gHSQC<sup>18</sup> experiments the spectral width was 10162.6 Hz in the  $F_2$  and 47998.2 Hz in  $F_1$ . The number of transients was 160 and 48 time increments were acquired with an acquisition time of 0.254 s. The data were zero filled to give a  $2 \times 8192 \times 256$  result. The HSQC pulse sequence was gradient enhanced.<sup>18</sup> The  $^1\text{H}$ – $^{15}\text{N}$  gHSQC correlations were performed using a one bond coupling constant of 89.9 Hz and multiple bond constants of 5 Hz. DMSO- $d_6$  (Euriso-top, 99.96% D) and DMF- $d_7$  (SDS, 99.50% D) solutions. In all the NMR experiments sample concentrations were in the range of  $3 \times 10^{-5}$  to  $3 \times 10^{-2}$  M. In the  $^1\text{H}$ – $^{15}\text{N}$  heteronuclear correlation measurements  $^{15}\text{N}$  chemical shifts are referenced to DMF- $d_7$  (SDS, 99.50% D,  $\delta_{\text{N}} = 104$  ppm) as internal standard. The reported chemical shifts for the  $^{15}\text{N}$  atoms were indirectly detected through the  $^1\text{H}$ – $^{15}\text{N}$  HMBC experiment.

Molecular mechanics calculations were performed using the 'Dreiding' force field,<sup>19</sup> with charge equilibration scheme using the interface Cerius2 (Molecular Simulations Inc.).

**Acknowledgment.** This project was supported by a grant of the Plan Nacional de I+D from the Ministerio de Ciencia y Tecnología of Spain.

**Supporting Information Available:** Peak assignment and spectra ( $^{13}\text{C}$  NMR,  $^1\text{H}$  NMR COSY and NOESY,  $^1\text{H}$ – $^{13}\text{C}$ , and  $^1\text{H}$ – $^{15}\text{N}$  HMBC and HSQC in DMSO- $d_6$  and DMF- $d_7$ ) of compounds **1** and **2**. This material is available free of charge via the Internet at <http://pubs.acs.org>.

JO011134D

(16) (a) Hurd, R. E. *J. Magn. Reson.* **1990**, *87*, 422–428. (b) Kienlin, M. V.; Moonen, C. T. W.; Toorm, A. V. D.; Zijl, P. C. M. V. *J. Magn. Reson.* **1991**, *93*, 423–429.

(17) (a) Bax, A.; Summers, M. F. *J. Am. Chem. Soc.* **1986**, 2093–2094. (b) Willrer, W.; Leibfritz, D.; Kerssebaum, R.; Bermel, W. *Magn. Reson. Chem.* **1993**, *31*, 287–292. (c) Ruiz-cabello, J.; Vuister, G. W.; Moonen, C. T. W.; Geldeven, P. V.; Cohen, J. C.; Zijl, P. C. M. V. *J. Magn. Reson.* **1992**, *100*, 282–303.

(18) (a) Kay, L. E.; Keifer, P.; Saarinen, T. *J. Am. Chem. Soc.* **1992**, *114*, 10663–10665. (b) Kontaxis, G.; Slhomehouse, J.; Lame, I. D.; Keeler, J. *J. Magn. Reson. Ser. A.* **1994**, *111*, 70–76.

(19) Mayo, S. L.; Olafson, B. D.; Goddard, W. A., III. *J. Phys. Chem.* **1990**, *94*, 8897–8909.